

ORIGINAL ARTICLE

HCN4 knockdown in dorsal hippocampus promotes anxiety-like behavior in mice

Anne Günther^{1,2}  | Vincent Luczak³  | Nadine Gruteser² | Ted Abel⁴  | Arnd Baumann² 

¹Laboratory for Synaptic Molecules of Memory Persistence, Center for Brain Science, RIKEN, Saitama, Japan

²Institute of Complex Systems, Cellular Biophysics (ICS-4), Research Center Jülich, Jülich, Germany

³Division of Biological Sciences and Center for Neural Circuits and Behavior, Neurobiology Section, Kavli Institute for Brain and Mind, University of California, San Diego, La Jolla, California, USA

⁴Iowa Neuroscience Institute, University of Iowa Carver College of Medicine, Iowa City, Iowa, USA

Correspondence

Anne Günther, Lab. Synaptic Molecules of Memory Persistence, RIKEN Center for Brain Science, Wako 351-0198, Japan.
Email: anne.guenther@riken.jp

Funding information

Directorate for Biological Sciences, Grant/Award Number: NSF 151548; National Science Foundation, Grant/Award Number: NSF 1515458

Hyperpolarization-activated and cyclic nucleotide-gated (HCN) channels mediate the I_h current in the murine hippocampus. Disruption of the I_h current by knockout of HCN1, HCN2 or tetratricopeptide repeat-containing Rab8b-interacting protein has been shown to affect physiological processes such as synaptic integration and maintenance of resting membrane potentials as well as several behaviors in mice, including depressive-like and anxiety-like behaviors. However, the potential involvement of the HCN4 isoform in these processes is unknown. Here, we assessed the contribution of the HCN4 isoform to neuronal processing and hippocampus-based behaviors in mice. We show that HCN4 is expressed in various regions of the hippocampus, with distinct expression patterns that partially overlapped with other HCN isoforms. For behavioral analysis, we specifically modulated HCN4 expression by injecting recombinant adeno-associated viral (rAAV) vectors mediating expression of short hairpin RNA against *hcn4* (shHcn4) into the dorsal hippocampus of mice. HCN4 knockdown produced no effect on contextual fear conditioning or spatial memory. However, a pronounced anxiogenic effect was evident in mice treated with shHcn4 compared to control littermates. Our findings suggest that HCN4 specifically contributes to anxiety-like behaviors in mice.

KEYWORDS

anxiety, elevated zero maze, fear conditioning, HCN channels, injection, locomotor activity, open field test, rAAV, rAAV9, RNAi, shRNA, spatial object recognition

1 | INTRODUCTION

Ion channels are the molecular basis of fast signal generation and propagation in neurons. One ion channel family uniquely contributing to neuronal signaling is the hyperpolarization-activated and cyclic nucleotide-gated (HCN) channels. In contrast to typical voltage-gated channels, HCN channels are not activated by membrane depolarization but by membrane hyperpolarization, and their activation kinetics can be modulated by direct binding of cyclic nucleotides.¹ Four homologous genes (*hcn1-4*) encoding isoforms of the HCN channel-forming subunits have been identified in mammals.²⁻⁴ These HCN isoforms (HCN1-4) display distinct biophysical characteristics and can arrange as homotetrameric and as heterotetrameric channels,⁵ giving rise to a variety of functional, biophysically diverse HCN channels. In addition to these pore-forming subunits, auxiliary subunits such as the tetratricopeptide repeat-

containing Rab8b-interacting protein (TRIP8b) modulate trafficking, targeting and gating of HCN channels.⁶⁻⁸ Additionally, HCN channel kinetics are modulated by numerous factors such as cyclic nucleotides, phosphorylation and interacting proteins.¹

In neuronal tissue, HCN channels mediate the hyperpolarization-activated (I_h) current, which was initially identified in pyramidal neurons of the hippocampal cornu ammonis1 (CA1) subfield.^{9,10} The I_h current is essential for controlling rhythmic activity in neuronal circuits (eg, in the thalamocortical system during the sleep-wake cycle) and also affects several essential constituents of neuronal processing such as resting membrane potentials, dendritic integration and synaptic transmission.¹¹ Studies at the mRNA and protein level showed that the four HCN isoforms display distinct expression patterns in the nervous system.¹²⁻¹⁴ Especially, notable was a pronounced HCN1 and HCN2 expression gradient along apical dendrites of CA1 pyramidal

This is an open access article under the terms of the Creative Commons Attribution-NonCommercial-NoDerivs License, which permits use and distribution in any medium, provided the original work is properly cited, the use is non-commercial and no modifications or adaptations are made.

© 2018 The Authors. Genes, Brain and Behavior published by International Behavioural and Neural Genetics Society and John Wiley & Sons Ltd.

neurons, increasing from proximal to distal. This gradient has been shown to substantially affect integration and temporal adjustment of synaptic inputs to CA1 pyramidal neurons.^{15–18}

Due to their diverging biophysical characteristics, HCN channels are likely candidates for directed modulation of hippocampal processing, as the individual isoforms differ strongly in for example, voltage dependence, activation kinetics and modulation by direct binding of cyclic nucleotides.¹ Notably, disruption of the I_h current by transgenic manipulation of HCN1, HCN2 or TRIP8b affects hippocampus-based behaviors including depression and anxiety.^{19–22} However, so far only the functional contribution of HCN1 and HCN2 to hippocampal processing has been described,^{22–24} while a potential role of HCN3 or HCN4 has not yet been addressed.

Notably, the biophysical characteristics of HCN4 differ strongly from other isoforms, with the most hyperpolarized midpoint of activation, the slowest activation kinetics and the most substantial cAMP-induced shift of activation toward depolarized potentials.²⁵ Transgenic mouse lines with impaired HCN4 expression have been used to show the importance of HCN4 in the context of cardiac pacemaking.^{26–29} However, reports on HCN4 expression in the murine hippocampus are scarce and not entirely consistent,^{14,30} and the effect of HCN4 disruption on hippocampal function has not been fully examined.

Here, we assessed the contribution of HCN4 to neuronal processing and hippocampus-based behaviors in mice. We examined the distribution of HCN4 using immunohistochemistry (IHC) and found that expression patterns of HCN4 largely resembled that of HCN1, but distinct differences were apparent at the subcellular level. For specific modulation of HCN4 expression, recombinant adeno-associated viral (rAAV) vectors mediating expression of short hairpin RNA against *hcn4* (shHcn4) were injected into the dorsal hippocampus of mice. Treatment with shHcn4 led to a reduction of *hcn4* transcript expression by about 60% compared to control-injected mice as well as a decrease of HCN4 protein expression. HCN4 knockdown produced no effect on contextual fear conditioning (FC) or spatial memory. However, a pronounced anxiogenic effect was evident in mice treated with shHcn4 compared to control littermates. In summary, HCN4 differs clearly from other HCN isoforms in its expression patterns as well as in its contribution to hippocampus-based behaviors.

2 | MATERIALS AND METHODS

2.1 | Antibodies

Primary and secondary antibodies used for IHC and western blot (WB) analysis are listed in the Supplementary Material (Table S1).

2.2 | Immunohistochemistry

Briefly, mice were transcardially perfused with ice-cold phosphate-buffered saline (PBS) followed by paraformaldehyde (PFA; 4% [w/v] in PBS) before dissection. Tissue was cryo-protected in 30% (w/v) sucrose, embedded in Tissue Tek (Sakura Finetek, Zouterwoude, The Netherlands), and coronal cryo-sections (30 μ m) were prepared. For IHC, sections were incubated in 0.3% (v/v) H_2O_2 for 30 minutes at room

temperature before unspecific binding sites were blocked for 1 hour in PBS containing 0.75% (v/v) Triton X-100, 5% (v/v) normal goat serum and 5% (v/v) normal donkey serum. Subsequently, primary antibodies were applied at 4°C for 3 days, and secondary antibodies were applied at room temperature for 4 hours (see Table S1). Fluorescent images were obtained with an inverted confocal microscope (TCS SP5II, Leica, Wetzlar, Germany) and analyzed using ImageJ software (ImageJ 1.46r, Wayne Rasband, US National Institutes of Health, Bethesda, Maryland).

2.3 | Constructs and rAAV preparation

Sequences containing the human U6 (hU6) promoter and shRNA constructs targeting the *hcn4* mRNA were purchased from Sigma-Aldrich (Taufkirchen, Germany). hU6-shRNA cassettes were cloned into the pENN-CaMKIIeGFP vector (provided by the University of Pennsylvania Vector Core), which encodes enhanced green fluorescent protein (eGFP) under the control of the neuron-specific calcium/calmodulin-dependent protein kinase II α (CaMKII α) promoter for monitoring of transduction efficacies. Viral particles were obtained from the University of Pennsylvania Vector Core or prepared in-house.

For in-house preparation, HEK293 cells (obtained from American Type Culture Collection; LGC Standards, Wesel, Germany) were triple-transfected with plasmids providing the recombinant viral genome (pENN-CaMKIIeGFP constructs) and the helper plasmids pRC³¹ (vector containing AAV *rep*- and *cap*-encoding regions) and pXX6-80.³² HEK293 cells were cultivated in DH10 medium (Dulbecco's Modified Eagle Medium + Glutamax [Invitrogen, Darmstadt, Germany], 10% (v/v) fetal bovine serum [FBS; Gibco/Thermo Fisher Scientific, Darmstadt, Germany], 1% (v/v) antibiotics/antimycotics [Invitrogen]) at 37°C, 5% CO₂ and 95% relative humidity. Medium was removed 24 hours after transfection and DH10 medium containing 2% (v/v) FBS was applied. After 24 hours, cells were harvested in 130-mM NaCl, 2.5-mM KCl, 1-mM MgCl₂, 70-mM Na₂HPO₄, and 30-mM NaH₂PO₄ (pH 7.4). Cells were lysed in 150-mM NaCl, 50-mM Tris/HCl (pH 8.5) in four freeze/thaw-cycles before digestion of nucleic acids with benzonase (50 U/mL; Merck Millipore, Darmstadt, Germany) for 30 minutes at 37°C.

Viral particles were enriched by density gradient centrifugation. The rAAV suspension was sublayered with iodixanol solutions (15%, 25%, 40% and 60% iodixanol; Sigma-Aldrich) and centrifuged (264,000 g, 4°C, 2 hours). Viral particles were collected in the 40% iodixanol phase and further purified using Amicon Ultra Centrifugal Filters (Ultracel-100 k, 15 mL; Merck Millipore). For determination of genomic titers, viral genomes were isolated using the DNeasy Blood & Tissue Kit (Qiagen, Hilden, Germany), and quantitative polymerase chain reaction (qPCR) was performed using primers framing a segment of the eGFP-encoding sequence (Table S2). Genomic titers were adjusted to 1×10^{10} genome copies per ml.

2.4 | Animals and stereotaxic injection

Animals were group-housed under standard conditions with access to food and water ad libitum in a 12-hour light-dark cycle. Experiments were carried out in accordance with National Institutes of Health guidelines and were approved by the University of Pennsylvania Institutional Animal Care and Use Committee. A total of 56 male

C57BL/6J mice (The Jackson Laboratory, Bar Harbor, Maine) were used. Mice received bilateral intrahippocampal injections of rAAV9 vectors or vehicle solution at 8 weeks of age. Stereotaxic injections were performed at anteroposterior -1.9 , mediolateral ± 1.5 and dorsoventral -1.4 from bregma using a 33-gauge beveled NanoFil needle, a NanoFil syringe and a MicroSyringe Pump Controller (World Precision Instruments, Sarasota, Florida). Viral suspension ($1 \mu\text{L}$) was infused at a rate of $0.2 \mu\text{L}/\text{min}$. After surgery, mice were single-housed and given 5 days to recover before pair housing.

2.5 | Quantification of gene expression by real-time polymerase chain reaction

Total RNA was isolated from dorsal hippocampal tissue after 3 to 8 wpi (weeks after injection). Briefly, tissue was lysed in $700\text{-}\mu\text{L}$ Qiazol Lysis Reagent using a stainless steel bead in a TissueLyser II (Qiagen). Proteins were removed using Phase Lock Gel tubes (5 Prime; QuantaBio, Beverly, Massachusetts) supplemented with $140\text{-}\mu\text{L}$ chloroform. RNA was isolated using the RNeasy Mini Kit (Qiagen). RNA samples were split for two independent first-strand cDNA syntheses using the RETROscript Kit (Ambion/Thermo Fisher Scientific).

Thermocycling was performed in a LightCycler 1.5 (Roche, Mannheim, Germany) using the QuantiTect SYBR Green polymerase chain reaction (PCR) Kit (Qiagen). Gene-specific primers (Table S2) were designed in silico and synthesized by MWG Operon (Ebersberg, Germany). Specificity and efficiency of primers was confirmed via BLAST analysis and semiquantitative PCR on hippocampal cDNA. In order to check for genomic impurities, *gapdh* primers were designed to bind in exons separated by an intron of 134 bp. qPCR reactions were performed on first-strand cDNA samples in a total volume of $20 \mu\text{L}$. Results were analyzed using the C_t method. Gene expression levels were normalized to the housekeeping gene *gapdh*.

2.6 | Quantification of protein expression by WB analysis

Total protein was isolated from dorsal hippocampal tissue after 3 to 8 wpi. Briefly, tissue was homogenized using a TissueRuptor (Qiagen), and proteins were solubilized in lysis buffer (150-mM NaCl, 5-mM ethylenediaminetetraacetic acid, 5-mM ethylene glycol tetraacetic acid, 1-mM dithiothreitol, $1\times$ Protease Inhibitor, 50-mM NaF, 0.1-mM NaVO_3 , 20-mM 4-(2-hydroxyethyl)-1-piperazineethanesulfonic acid, 1% octylphenoxy poly(ethyleneoxy)ethanol, pH 7.4). Proteins were separated on Criterion 4%-20% gradient gels (Bio-Rad, Hercules, California) using the NuPAGE buffer system (Life Technologies/Thermo Fisher Scientific). Proteins were transferred in blotting buffer (192-mM glycine, 20% methanol, 3-mM sodium dodecyl sulfate (SDS), 25-mM Tris/HCl, pH 7.6) onto ImmunBlot polyvinylidene fluoride membranes (Bio-Rad).

For WB analysis, unspecific binding sites were blocked in 5% (w/v) low-fat milk in tris-buffered saline with tween-20; (TBST; 50-mM Tris, 150-mM NaCl, 0.02% (v/v) Tween-20, pH 7.6). Membranes were incubated with primary antibodies, washed with TBST and incubated with horseradish peroxidase (HRP)-coupled secondary antibodies (see Table S1). Immunoreactive protein bands were

detected using a Chemiluminescence Detection Kit for HRP (AppliChem, Darmstadt, Germany) and ImageQuant LAS 4000 technology (GE Healthcare, Pittsburgh, Pennsylvania). For reprob- ing of WBs, bound antibodies were removed by incubation in stripping buffer (Thermo Fisher Scientific, Waltham, Massachusetts).

2.7 | Behavioral paradigms

The contribution of HCN4 to hippocampus-dependent behavioral paradigms was assessed using three groups of mice. Behavioral tests proceeded from the least to the most stressful test for the animals (Figure S1). Data from different groups were combined for statistical analysis. Behavioral testing and tissue collection were performed during the light phase.

2.7.1 | Elevated zero maze test

Naïve pair-housed mice were exposed to a Plexiglas elevated zero maze (EZM) with a width of 5 cm and an outside circumference of 200 cm, arranged in two open and two closed quadrants. For behavioral testing, animals were allowed to freely explore the arena for 5 minutes and sessions were recorded digitally. Automated scoring software (MATLab ZeroMaze; <https://www.seas.upenn.edu/~molneuro/autotyping.html>, v14.08, Neurobehavior Testing Core, University of Pennsylvania, Pennsylvania) was used for analysis.³³

2.7.2 | Open field test and locomotor activity measurement

Mice were exposed to light beam-equipped open field chambers ($55 \text{ cm} \times 55 \text{ cm}$) and allowed to explore freely for 10 minutes. Sessions were recorded digitally and scored using automated MATLab OpenField (<https://www.seas.upenn.edu/~molneuro/autotyping.html>, v14.08, Neurobehavior Testing Core, University of Pennsylvania) software.³³ For analysis, quadrants were defined as center (greater than 5 cm from arena wall) and peripheral (within 5 cm of arena wall) zones. Additionally, light beam crossings were recorded for locomotor activity (horizontal crossings) and rearing (vertical crossings).

2.8 | Statistical analysis

All data are given as mean \pm SEM (SE of the mean). The two-tailed unpaired Student's *t* test was used to calculate *P*-values for analysis of gene expression as well as mouse behavior during the EZM test, the open field test (OFT) and the spatial object recognition (SOR) test. Two-way ANOVA with replication was applied for analysis of locomotor activity and contextual FC. For all behavioral experiments, animals showing responses two SDs above or below the group mean were excluded from the analysis as statistical outliers. Analysis of behaviors without outlier exclusion is included in the supplementary. A *P*-value of <0.05 was considered significant.

3 | RESULTS

3.1 | Expression of HCN4 in hippocampal tissue

All four HCN isoforms are expressed in the murine central nervous system (CNS), but their precise distribution has been shown to differ distinctly depending on the examined CNS region.¹¹ Generally, HCN1 and HCN2 are the predominantly expressed isoforms, and their function in neuronal signaling has been studied in detail, whereas little is known about the roles of HCN3 and HCN4. Here, we focused on the specific contribution of HCN4 to hippocampus-based behaviors. In a first step, expression profiles of all four HCN isoforms were examined in hippocampal tissue on the RNA and protein level.

Specific primers were used to amplify defined fragments of individual *hcn* isoforms (Table S2). Specificity and efficiency of these primer pairs was confirmed by BLAST analysis and semiquantitative PCR on mouse brain cDNA (Figure S2). Transcript expression levels of *hcn* genes in murine hippocampal tissue were quantified by qPCR and normalized to *gapdh*. As shown in Figure 1A, the amount of *hcn4* transcripts was much lower than that of *hcn1* and *hcn2* (Figure 1A), while *hcn3* transcripts were barely detectable (not shown). Protein expression of HCN isoforms was examined on WBs (Figure 1B). WB results largely confirmed qPCR data, with strong expression of HCN1 and HCN2 and much lower expression of HCN4. Expression of HCN3 could not be detected on WBs (data not shown).

Using immunohistochemical (IHC) staining on hippocampal tissue sections with HCN isoform-specific primary antibodies, the cellular localization of HCN isoforms was examined. Several monoclonal and polyclonal antibodies were applied for labeling of individual isoforms (Table S1). Expression of HCN1, HCN2 and HCN4 was confirmed throughout the hippocampal formation (Figure 1, C1-C4). As already indicated by qPCR and western blotting, HCN4 protein expression was lower than that of HCN1 and HCN2, but distinct HCN4 expression patterns could be detected throughout the hippocampus along the dorsoventral axis (Figure S3A). Notably, we observed an expression gradient of HCN4 along the dendrites of CA1 pyramidal neurons (Figure 1C4), a pattern which has previously only been reported for the HCN1 and HCN2 isoforms.^{16,17}

We also identified additional distribution patterns for the individual HCN isoforms on the subcellular level. The HCN2 isoform was expressed in a distinct population of cells (Figure 1, D3-F3), which have previously been classified as interneurons.^{23,36} Both, HCN1 and HCN4 appeared in punctate structures throughout the cell body layer of the dentate gyrus (DG) and the CA regions (Figure 1, C2/4-F2/4).

Higher magnification of coimmunostained sections showed that most HCN4-positive structures were also stained by HCN1-specific antibodies (Figure 1G). Notably, the presence of different HCN isoforms might indicate the possibility of the formation of heterotetrameric channels in these subcellular structures, which remains to be assessed in forthcoming studies. In addition to costained structures, we detected an even higher number of punctae that contained HCN1 but not HCN4 (Figure 1G).

In order to assess the subcellular localization of HCN1 and HCN4, we performed a series of IHC stainings with antibodies specific for the individual HCN isoforms and for molecular markers of synaptic

substructures (Figure S3, B-I). Coimmunostaining with glutamate decarboxylase (GAD65/67), a marker of the inhibitory pre-synapse, showed an overlap with HCN1-positive structures, whereas no colocalization with HCN4 was found (Figure S3, D-F). In contrast to these results, coimmunostaining HCN isoforms and Homer-1, a marker of excitatory post-synapses, showed no structures costained for Homer-1 and either HCN1 or HCN4 (Figure S3, C/G/H). Thus, despite the overall similar expression patterns of HCN1 and HCN4 in hippocampal tissue, we observed clearly distinct localizations of these isoforms on the subcellular level. These results emphasize the precise and differential targeting of individual HCN isoforms to distinct subcellular structures.

In summary, relatively high levels of HCN1 and HCN2 are expressed in murine hippocampal tissue at the mRNA and protein level, while HCN4 expression is much lower. We found partially overlapping expression patterns for HCN1 and HCN4. However, at the subcellular level clear differences were apparent, including a higher number of HCN1-positive vs HCN4-positive structures as well as association between GAD65/67-stained and HCN1-stained but not HCN4-stained structures.

3.2 | Specific knockdown of HCN4 in dorsal hippocampus

Based on our IHC results, we hypothesized that HCN1 and HCN4 might contribute to similar hippocampus-dependent behavioral processes. While transgenic approaches allow comprehensive analysis of protein function in physiological contexts, transgenic manipulation of HCN4 is problematic as it can lead to embryonic lethality due to cardiac dysfunction.²⁶⁻²⁹ Previously, a lentivirus-based approach showed that knockdown of *hcn1* restricted to the dorsal hippocampal CA1 region in rats resulted in antidepressant and anxiolytic-like behaviors.¹⁹ Thus, we applied rAAV vectors by stereotaxic injection, to express HCN4-specific short hairpin RNAs (shRNA) in the dorsal hippocampus of mice to gain insight into a possible contribution of HCN4 channels to mouse behavior (Figure 2A).

Viral vectors applied in this study were designed to mediate simultaneous expression of shRNAs under the control of the constitutive hU6 promoter and of eGFP under the control of the neuron-specific CaMKII α promoter (Figure 2B). The sequence of the HCN4-specific shRNA construct (shHcn4) was targeted to the exon encoding the HCN4 C-terminus (Figure 2C). Several shRNA constructs targeting different segments of the *hcn4* gene were tested in vitro on HCN4-expressing cell lines in order to identify shRNAs that mediate specific and efficient downregulation of HCN4 expression. The most promising shRNA construct (shHcn4) binds to the exon encoding the HCN4 C-terminus (Figure 2C). For in vivo application, rAAV vectors were injected into the dorsal CA1 region of 4-week-old mice. Strong expression of eGFP was detected at 3 wpi throughout the dorsal hippocampus (Figure 2D). Expression of eGFP remained for at least 8 wpi (data not shown).

Quantification of transcript levels by qPCR showed a reduction of *hcn4* mRNA in dorsal hippocampal tissue of animals treated with rAAV-shHcn4 (Figure 3). Compared to control samples, *hcn4* transcript levels were reduced by about 60% (Figure 3A; $t[10] = 9.92$,

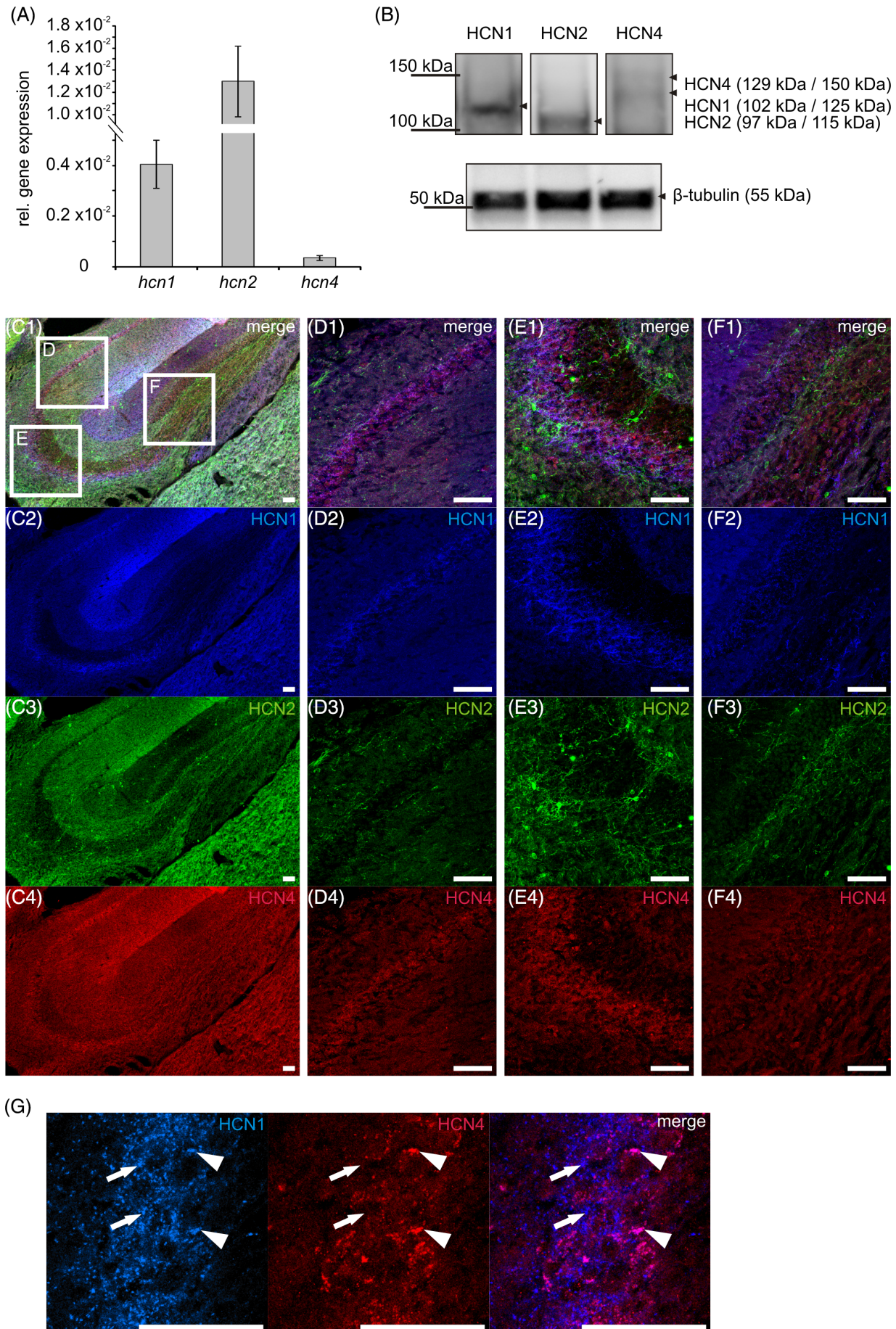


FIGURE 1 Legend on next page.

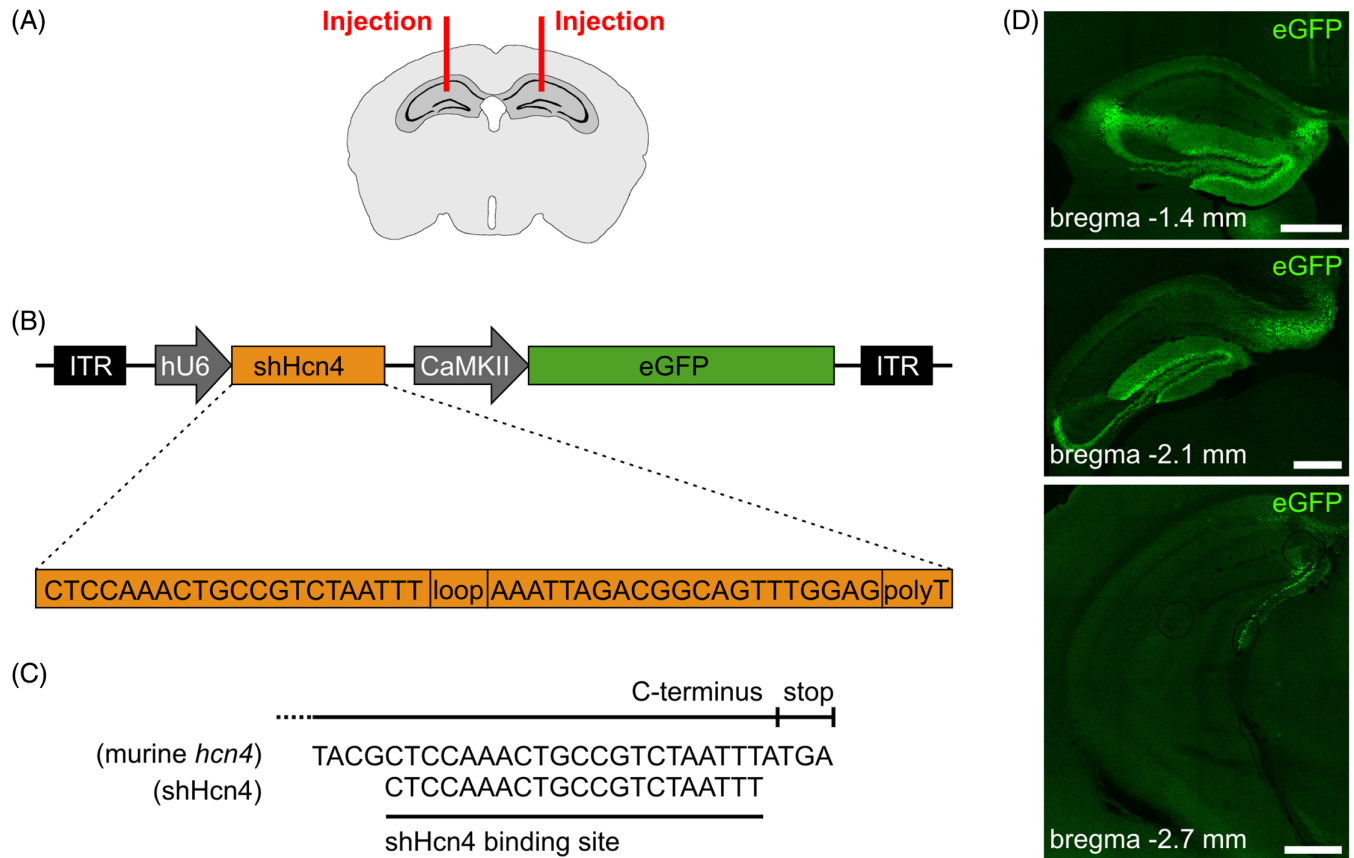


FIGURE 2 Injection of shHcn4-expressing rAAV9 vectors into the dorsal hippocampus. A, Scheme of the bilateral stereotaxic injection into the dorsal hippocampus at bregma -1.9 mm is shown. B, Schematic representation of the shHcn4-encoding viral genome. Sequence elements are indicated by colored bars. Viral vectors were designed to encode eGFP under the control of the neuron-specific CaMKII α promoter and shRNA sequences under the control of the hU6 promoter. The shRNA expression cassettes were placed upstream of the eGFP expression cassette. Constructs are flanked by inverted terminal repeats for viral packaging. A shHcn4 sequence is shown including the loop hairpin segment and the polyT signal sequence segment. C, Alignment of the 21 bp shHcn4 sequence on murine *hcn4* mRNA is shown. D, Hippocampal eGFP expression (green) at 3 wpi is shown. After a single injection of rAAV-shHcn4 at bregma -1.9 mm, eGFP expression spread along the hippocampal axis. Antero-posterior positions are indicated for individual images. Bars specify 500 μ m

$P < 0.001$). We did not observe an effect on *hcn1* or *hcn2* transcript levels (Figure S4A).

Western blotting was used to examine HCN4 knockdown efficiency at the protein level. Total protein was isolated from dorsal hippocampal tissue of mice injected with rAAV-shHcn4 or with control (rAAV-eGFP control vector or vehicle PBS). Two bands were detected with an HCN4-specific antibody (Figure 3B), corresponding to glycosylated and nonglycosylated HCN4 protein.^{34,37–39} Compared to control samples, the intensity of these bands was reduced in rAAV-shHcn4-treated samples (Figure 3B). Consistent with qPCR results, application of rAAV-shHcn4 did not affect HCN1 or HCN2 protein expression levels

(Figure S4B). Notably, no eGFP expression was detected in ventral hippocampal tissue isolated from the same animals (Figure S4C).

For IHC analysis, sections of tissue unilaterally injected with rAAV-shHcn4 and contralaterally injected with PBS were stained using HCN4-specific antibodies. eGFP autofluorescence confirmed injection and transduction of dorsal hippocampal tissue with rAAV. No eGFP fluorescence was detected in the PBS-injected contralateral hippocampus. Expression of HCN4 was clearly reduced in shHcn4-treated regions compared to control tissue (Figure 3C).

In order to assess possible adverse or inflammatory responses to treatment with shRNA-encoding rAAV, we monitored expression of

FIGURE 1 HCN isoform expression in dorsal hippocampal tissue. A, Relative expression of *hcn1*, *hcn2* and *hcn4* was determined by qPCR. Transcript levels of *hcn* genes were normalized to *gapdh* transcript levels. Data are given as mean \pm SEM ($n = 4$). B, Expression of HCN1, HCN2 and HCN4 protein was assessed on WBs. Positions and molecular weights of marker proteins are indicated on the left. Protein bands are indicated for HCN1, HCN2, HCN4 and β -tubulin by arrowheads on the right. Molecular weights are given in parentheses as calculated molecular weight/glycosylated HCN subunit (HCN1: 125 kDa; HCN2: 115 kDa; HCN4: 150 kDa^{34,35}). (C–G) Immunohistochemical analysis of sagittal sections is shown for HCN1 (blue), HCN2 (green) and HCN4 (red). Proteins were stained with specific primary antibodies and fluorescently labeled secondary antibodies (see Table S1). Samples were examined by confocal microscopy. An overview of the hippocampus is shown on the left (C1–C4). Positions of higher magnification images are indicated by white frames, depicting the CA1 region (D1–D4), the CA3 region (E1–E4) and the DG (F1–F4). High magnification of HCN1 and HCN4 staining in the CA3 region is shown in (G). Arrows indicate HCN1-positive structures, arrowheads indicate structures positive for both HCN1 and HCN4. Bars specify 50 μ m

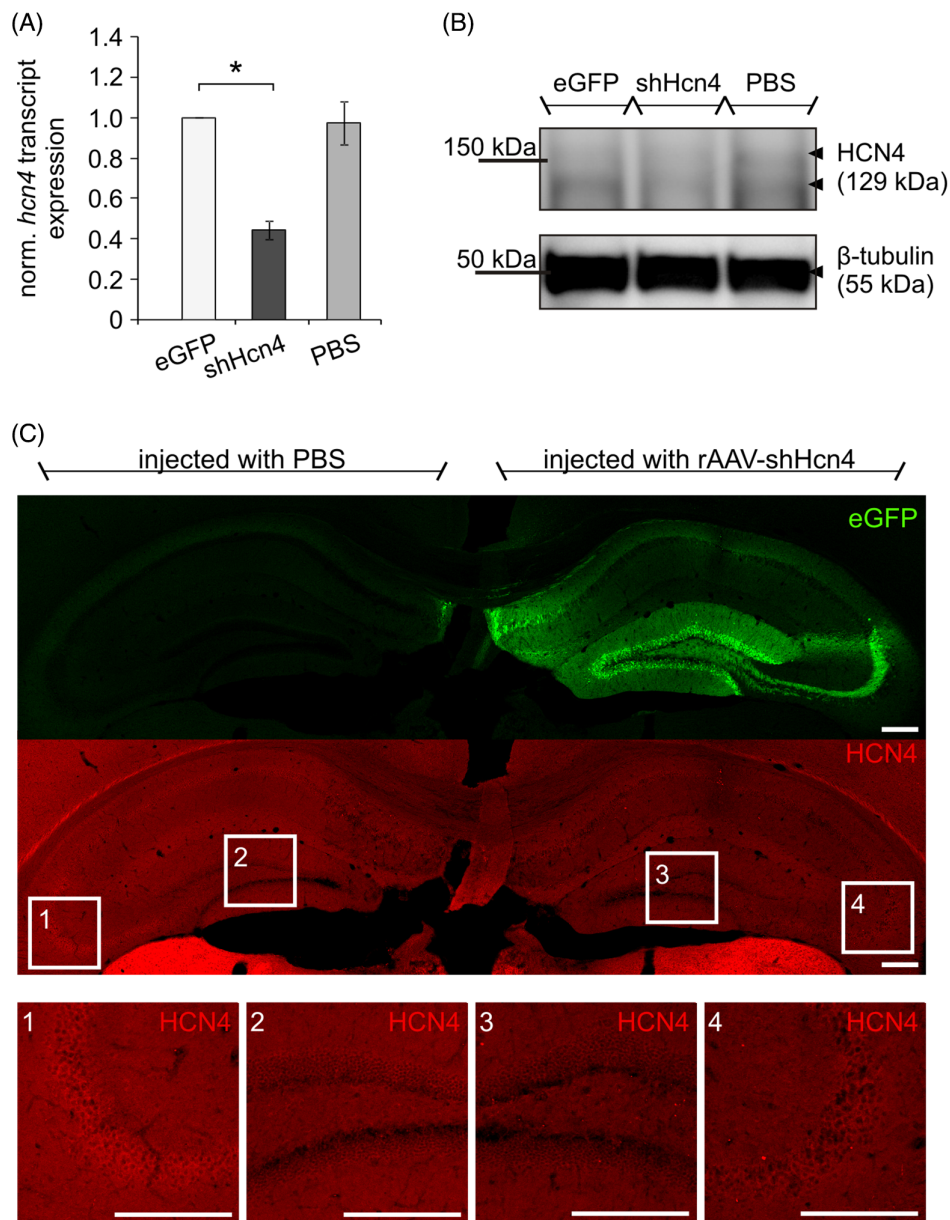


FIGURE 3 Specific knockdown of HCN4 in the dorsal hippocampus. Mice were injected with rAAV-shHcn4 (shHcn4) and as control either with rAAV-eGFP (eGFP) or with PBS. Tissue was analyzed at 3 wpi. A, Quantitative PCR analysis is shown for *hcn4* transcripts. First-strand cDNA was synthesized on total RNA isolated from eGFP-treated, shHcn4-treated and PBS-treated dorsal hippocampal tissue. Efficiency-corrected relative expression was calculated. Values are mean \pm SEM (eGFP: $n = 6$; shHcn4: $n = 6$; PBS $n = 4$). B, WB analysis of HCN4 knockdown in dorsal hippocampal tissue. Treatment of tissue is specified above lanes. After staining with specific antibodies, signals were detected using enhanced chemiluminescence. Positions and molecular weights of marker proteins are indicated on the left. Protein bands are indicated for HCN4 and β -tubulin by arrowheads on the right and their calculated molecular weights are given in parentheses. C, For immunohistochemical analysis, mice were unilaterally injected with rAAV-shHcn4 (shHcn4). The contralateral hippocampus received a PBS injection (control). Both hippocampi are shown with eGFP autofluorescence (green) and specific immunohistochemical staining of HCN4 (red). The lower panel shows higher magnification images of HCN4 immunoreactivity in areas indicated by white frames. Images 1 and 2 show areas representative for the PBS-injected hippocampus. Images 3 and 4 show similar areas of the contralateral hippocampus injected with rAAV-shHcn4. Bars specify 250 μ m

glial fibrillary acidic protein (GFAP) as a marker for astrogliosis and activated caspase-3 (Casp-3) as a marker for apoptosis.⁴⁰ No increased expression of GFAP or Casp-3 was apparent in immunohistochemically stained tissue sections (Figure S5A) or on WBs (Figure S5B), when comparing shHcn4-treated tissue to control tissue.

In summary, these results confirm specific knockdown of the HCN4 isoform on the RNA and protein level, induced by a single infusion of rAAV-shHcn4 and restricted to the dorsal hippocampal region. We did not observe off-target effects on gene expression of either

homologous HCN isoforms or on markers for inflammatory tissue responses.

3.3 | Knockdown of HCN4 did not alter locomotor activity

In order to assess the contribution of HCN4 to mouse behavior, animals were bilaterally injected with rAAV and tested in several behavioral paradigms (see Figure S1).

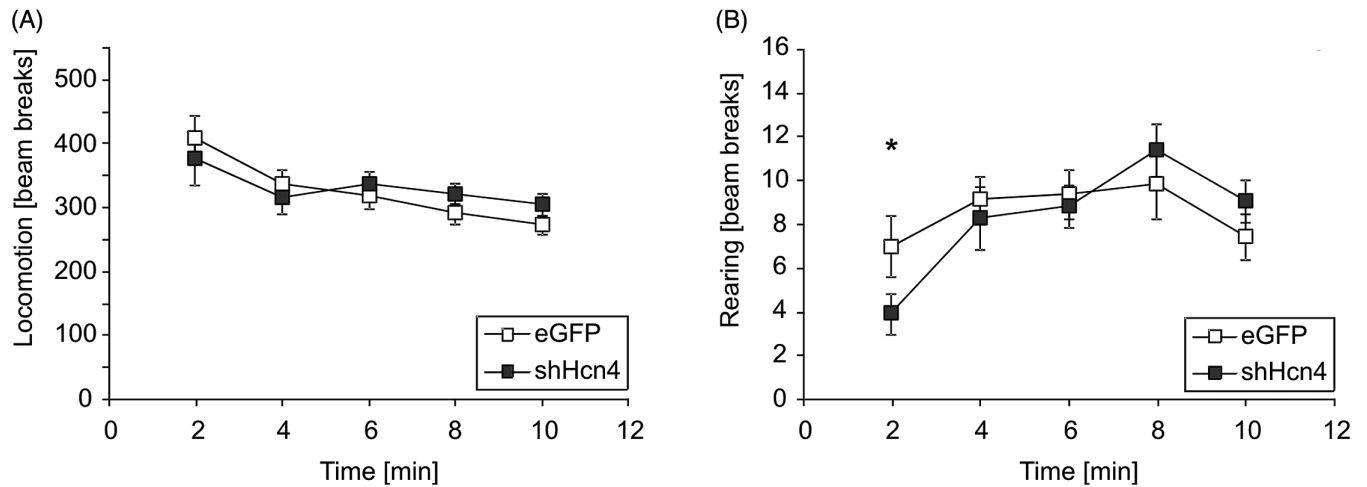


FIGURE 4 Locomotor activity and rearing behavior of shHcn4-treated and control mice. Locomotion and rearing behavior of mice treated with rAAV-shHcn4 (shHcn4) or rAAV-eGFP (eGFP) is shown. A, Locomotion was analyzed as horizontal light beam breaks in 2-minute intervals in a testing session of 10 minutes. B, Rearing behavior was analyzed as vertical light beam breaks in 2-minute intervals in a testing session of 10 minutes. Values are mean \pm SEM (eGFP, shHcn4: $n = 16$)

First, we assessed effects of HCN4 knockdown on overall locomotion in automated open field arenas equipped with light beams (Figure 4, S6). Light beam crossings were recorded and averaged in 2-minute intervals over a total test period of 10 minutes. Locomotor activity for shHcn4-treated mice and control littermates decreased over time, and no significant difference was observed between the groups (Figure 4A). Exploratory behavior was evaluated based on rearing. No difference of rearing behavior was observed between groups, except for the first 2-minute interval, where shHcn4-treated mice showed significantly less rearing than control animals (Figure 4B; $t[29] = 2.21, P < 0.04$).

3.4 | Anxiogenic effect of HCN4 knockdown in the dorsal hippocampus

Previous studies have addressed the effects of I_h current disruption on anxiety-related behaviors, but the results of these studies were not entirely consistent.^{19,20,22} Thus, in this study, we examined whether HCN4 knockdown affects anxiety in mice.

Mice treated with rAAV-shHcn4 or control virions were tested in the EZM to assess anxiety levels (Figure 5, S7). The arena is schematically depicted in Figure 5A. Compared to control mice, shHcn4-treated mice spent more time in the closed arms of the EZM (Figure 5B; $t[42] = 2.91, P < 0.006$). Additionally, shHcn4-treated mice showed significantly less ambulation (Figure 5C; $t[41] = 3.96, P < 0.003$) as well as significantly less transitions between open and closed arms (Figure 5D; $t[40] = 3.56, P < 0.001$). These results suggest an anxiogenic effect of HCN4 knockdown.

Subsequently, the OFT was applied to examine whether this anxiogenic effect of HCN4 knockdown in the EZM was consistent in other anxiety-related paradigms (Figure 5, S7). The arena is also schematically depicted in Figure 5A. Notably, the observed anxiogenic effect persisted in the OFT, with shHcn4-treated animals spending significantly more time at the periphery of the open field arena compared to control mice (Figure 5E; $t[28] = 3.2, P < 0.004$). Overall ambulation was unaffected by HCN4 knockdown (Figure 5F).

3.5 | No effect of HCN4 knockdown on spatial memory or fear memory

In order to determine whether HCN4 knockdown affects other hippocampus-based behaviors, we assessed spatial memory as well as contextual fear memory in shHcn4-treated mice and control littermates. Spatial memory was tested using an SORTask. No significant difference of object exploration time for displaced and nondisplaced objects was observed when comparing mice treated with rAAV-shHcn4 or with rAAV-eGFP control (Figure S8).

Contextual fear memory was assessed using contextual FC. No significant difference of freezing levels was detected for shHcn4-treated mice compared to eGFP-treated littermates before or after applying a footshock of 0.75 mA (Figure S9A) or 1.5 mA (Figure S9B) for 2 seconds. We also tested the same animals in different paradigms of fear extinction and retrieval, but no significant differences were apparent between groups (Figure S9). However, rAAV-shHcn4-treated mice reliably showed slightly higher freezing levels than control-treated littermates during the 24-hour test as well as lower freezing levels during extinction, although this result did not reach statistical significance (Figure S9).

Taken together, the results of this study showed a specific and reproducible anxiogenic effect of HCN4 knockdown in the dorsal hippocampus, without affecting other hippocampus-based behaviors.

4 | DISCUSSION

The HCN-mediated I_h current modulates cellular membrane properties and plays an essential role in hippocampal signal processing.¹¹ Here, we specifically addressed the contribution of the HCN isoform 4 to hippocampus-based behaviors. Using IHC, we observed distribution patterns of HCN4 in the hippocampal formation that partially overlapped with those of HCN1 and HCN2. However, HCN4 expression levels were consistently lower compared to these two isoforms in hippocampal neurons. Overlapping expression between HCN4 and

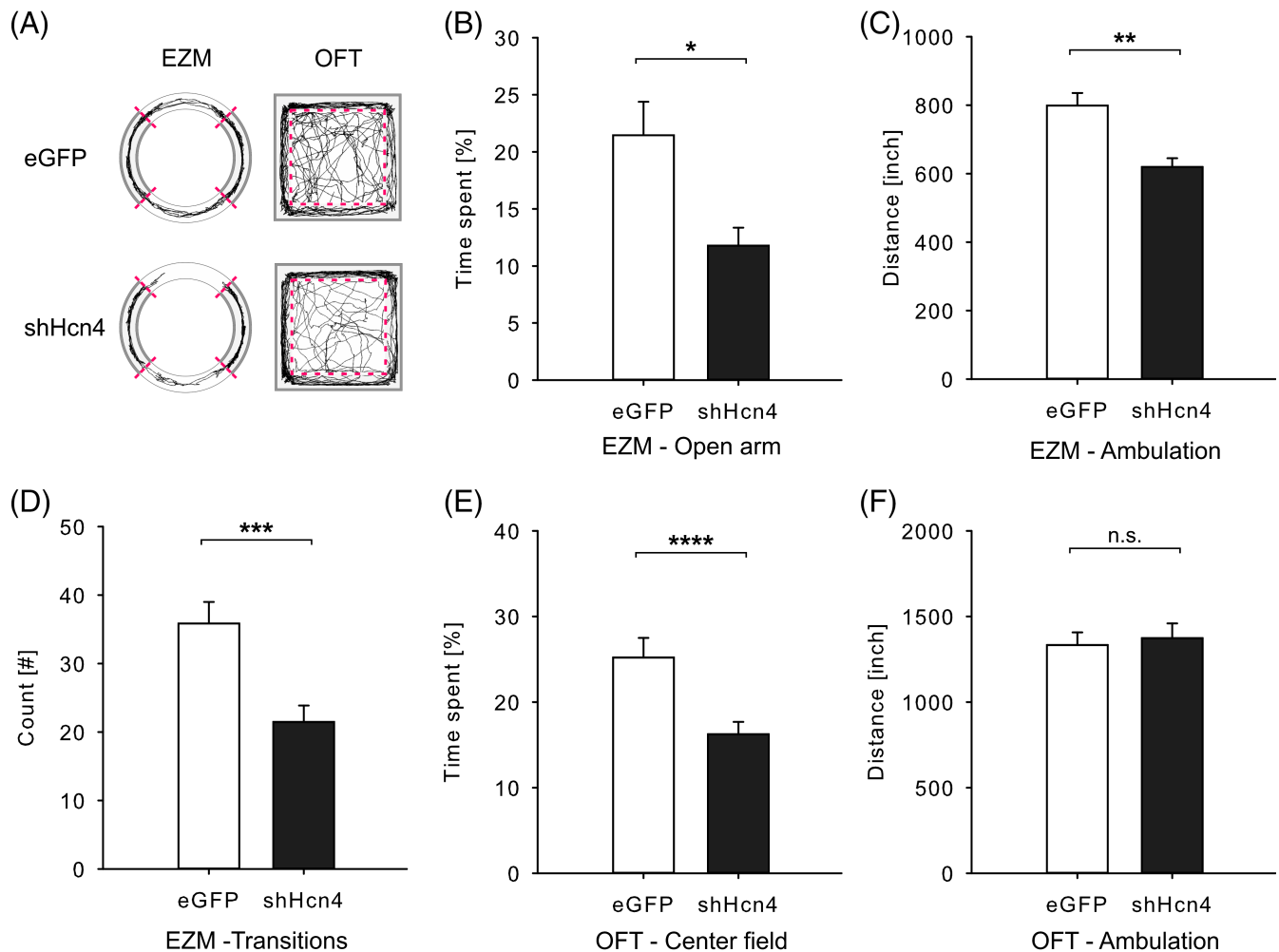


FIGURE 5 Effect of HCN4 knockdown on anxiety-like behavior. A, Representative tracking images during EZM and OFT of mice treated with rAAV-shHcn4 (shHcn4) or rAAV-eGFP (eGFP) are shown. For EZM, time spent in open arms (B), total ambulation (C) and number of transitions between open and closed arms (D) were analyzed (EZM: eGFP $n = 21$; shHcn4 $n = 24$). For OFT, time spent in the center field (E) and total ambulation (F) were analyzed (OFT: eGFP, shHcn4 $n = 15$). Values are given as mean \pm SEM

HCN1 isoforms was especially evident in a subset of synaptic contacts in the cell body layer of CA regions. Notably, it has been shown that presynaptic HCN channels facilitate transmitter release,¹¹ whereas postsynaptic HCN channels reduce temporal summation of postsynaptic potentials.^{6,41} Thus, HCN channels can have a strong impact on neuronal signaling at the subcellular level. Here, we observed an expression gradient of HCN4 along the dendrites of CA1 pyramidal neurons, similar to the previously described gradient for the HCN1 and HCN2 isoforms.^{15,18} These expression gradients of HCN isoforms are physiologically reflected as a 6-fold increase of I_h current densities from the soma to the distal dendrite. These current density profiles affect integration and temporal adjustment of synaptic inputs in CA1 pyramidal neurons.^{16,17}

An essential aspect of HCN channel physiology is the distinct biophysical properties of the four individual HCN isoforms, which combined with their ability to form homotetramers as well as heterotetramers gives rise to a wide range of functional but biophysically diverse HCN channels.⁵ Notably, HCN1 and HCN4 show the most divergent properties of the four isoforms, with for example, HCN4 displaying the slowest and HCN1 the fastest time constant of

activation. Furthermore, HCN4 has the most hyperpolarized midpoint of activation ($V_{0.5} \approx -100$ mV) and HCN1 the most depolarized ($V_{0.5} \approx -70$ mV).^{1,42} Additionally, the activation curve of HCN4 can be strongly shifted toward more depolarized potentials by direct binding of cAMP and by Src kinase phosphorylation, whereas HCN1 activation is only slightly modulated by cAMP and not affected by Src kinase.²⁵ Our results in hippocampal tissue show partial overlap of HCN1, HCN2 and HCN4 expression, implying the presence of biophysically and functionally distinct I_h currents in the same subcellular structures. It remains to be addressed electrophysiologically whether homotetrameric or heterotetrameric HCN channels are present in the different HCN-positive structures of hippocampal neurons.

In order to gain insight on the functional contribution of HCN4 to hippocampus-based behavioral processes, we applied a virus-based shRNA-mediated gene knockdown approach. Due to the crucial role of HCN4 in cardiac pacemaking during embryonic development, conventional transgenic approaches for disruption of the *hcn4* gene can result in lethality in utero.^{27–29} Notably, even in adult animals, HCN4 retains an important role in the maintenance of normal heart rhythmicity.²⁶ Therefore, we used stereotaxic injection of rAAVs to induce

specific downregulation of HCN4 expression in a temporally defined and spatially restricted manner.

We employed AAV serotype 9, which provides anterograde and retrograde transport in neurons.⁴³ A single infusion of eGFP-encoding rAAV resulted in strong expression of the fluorescent marker protein throughout the dorsal hippocampus and remained restricted to hippocampal tissue for several weeks.

Application of rAAV-shHcn4 reduced HCN4 expression at the mRNA level (by about 60%) as well as at the protein level. Here, disruption of HCN4 expression produced pronounced anxiogenic effects in two independent behavioral paradigms for anxiety, the EZM⁴⁴ and the OFT.⁴⁵ Mice treated with rAAV-shHcn4 spent less time in the open arms of the EZM and less time in the center of the open field. Overall locomotion of the animals was unaffected, thus excluding effects on motor activity as the explanation for the observed anxiogenic behaviors. Currently, available phenotypic data (International Mouse Phenotyping Consortium, <http://www.mousephenotype.org/data/genes/MGI:1298209>) suggests a slight effect in heterozygous knockout animals in the open field, concurring with the results of this study. A hippocampal region-specific, homozygous *hcn4* knockout strategy, would give even further insight into the role of HCN4 in anxiety-related behaviors. Several studies have reported effects of I_h current disruption on anxiety-related and depression-related behaviors, although results are not consistent. Mice lacking HCN1 or HCN2 have been reported to display antidepressant-like behaviors but unchanged anxiety-related behaviors.^{20,22} Conversely, region-specific knockdown of HCN1 in the dorsal CA1 region of rats was shown to lead to both anxiolytic as well as antidepressant behaviors.¹⁹ Therefore, the results of our study indicate that HCN4 might play an opposing role to HCN1 in anxiety-related behaviors.

Due to their high sensitivity toward cyclic nucleotides, HCN4 channels might also play a particular role in cAMP-modulated signal relay cascades, which are essential during hippocampal processing. In the presence of cAMP, the midpoint of activation shifts by up to 25 mV toward more depolarized potentials.¹ Studies on knockout mice lacking specific phosphodiesterase isoforms have shown that the resulting elevated intracellular cAMP levels promote anxiogenic effects.^{46,47} This biochemical effect might be mediated via HCN channel activity resulting in physiological and behavioral responses. A possible explanation for this effect is a shift of I_h current activation toward more depolarized potentials caused by cAMP binding to HCN channel subunits. Similarly, interfering with $\alpha 2A$ -adrenergic receptor expression in the prefrontal cortex has been reported to affect HCN channel activation, resulting in altered neuronal activity and anxiety-related behaviors,^{48,49} which may also result from shifting the activation kinetics of HCN channels and thereby directly affecting neuronal activity.⁵⁰

An essential contributor to HCN physiology is the auxiliary subunit TRIP8b, which affects trafficking as well as biophysical properties of HCN channels in several areas of the CNS.^{51–55} In hippocampal neurons, downregulation of TRIP8b alters I_h current density⁵⁴ and the resulting disruption of both synaptic and intrinsic plasticity of I_h current during activity⁵¹ results in antidepressant-like behaviors.²⁰ Notably, this effect is bidirectional as TRIP8b rescue can restore normal HCN channel trafficking and normal behaviors.⁵² The integral role of TRIP8b in HCN channel regulation is further emphasized by its effect on the overall protein

expression of HCN channels in different areas of the CNS^{52,53,55} as well as on the basal cAMP levels in brain tissue.⁵⁵ Notably, the modulating effects of TRIP8b differ depending on the principal, channel-forming HCN isoform. It has been shown that binding of TRIP8b impairs cAMP effects on HCN2 and HCN4 but does not affect cAMP modulation of HCN1.⁵⁶ While binding affinities of cAMP to all four subunits show pronounced cooperativity,⁵⁷ this allosteric effect gains further complexity as cAMP and TRIP8b directly compete for binding to the HCN cyclic nucleotide-binding site (CNBD).^{53,58,59} Furthermore, the two distinct sites for interaction of TRIP8b with the HCN C-terminus and the CNBD have been shown to differentially affect HCN trafficking and gating.^{58,59} Additionally, TRIP8b regulates trafficking and modulation of HCN isoforms in a TRIP8b splice variant-dependent,^{7,8,54} highly compartment-selective⁶ and even age-dependent⁶⁰ manner. Studies have shown direct interaction of TRIP8b and HCN4⁵⁶ as well as reduction of HCN4 expression due to TRIP8b knockout in thalamic tissue.^{53,55} Especially, the strong effect of TRIP8b on neuronal activity and behaviors in the thalamus^{53,55} suggests a direct functional effect of TRIP8b and HCN4 favored by the strong expression of HCN4 in thalamic tissue. Thus, TRIP8b might be essential for differentially modulating the functional contribution of individual HCN isoforms in hippocampal processing.

While the effect of I_h current disruption on spatial memory is conversely discussed, studies agree that disruption of HCN1, HCN2 or TRIP8b does not affect contextual FC.^{20,22} In our study, knockdown of HCN4 in the dorsal hippocampus had no effect on overall performance in SOR tasks as well as in behavioral paradigms assessing contextual fear memory and fear extinction. Therefore, HCN4 does not appear to be a critical component for hippocampus-based memory processes. Our results strongly emphasize a specific role of HCN4 in anxiety-related behaviors.

Our findings of low HCN4 expression in several areas of the hippocampus, partially overlapping with the predominant HCN1 and HCN2 isoforms, supports the hypothesis of HCN4 not being a main constituent of hippocampal I_h currents. Nevertheless, due to its distinct biophysical properties, the HCN4 isoform could serve to diversify native I_h currents by forming heterotetrameric channels in hippocampal cells, possibly even in an activity-dependent manner. An essential aspect of future studies will be the dissection of subregion-specific effects of HCN channels modulating hippocampal processes. Using virus-mediated RNAi-based approaches for simultaneous knockdown of HCN isoforms will allow electrophysiological and behavioral dissection of the specific contribution of individual HCN isoforms to hippocampal processes. All in all, the findings of this study give additional insight into the molecular mechanisms underlying the dynamic regulation of anxiety-related behaviors. Especially, the contrast between the findings for HCN4 in this study and the reported results for HCN1 in the context of anxiety-related behaviors suggest HCN4 as a potential therapeutic target for treating anxiety.

ACKNOWLEDGMENT

We gratefully acknowledge the assistance of Dr. H. Büning (Center for Molecular Medicine Cologne, Cologne, Germany) with establishing the rAAV cell culture. We thank Dr. F. Müller (Research Center Jülich, Jülich, Germany), Dr. A. Mataruga (Research Center Jülich, Jülich,

Germany) and Dr. E. Kremmer (Helmholtz Center Munich, Munich, Germany) for providing HCN isoform-specific antibodies. T.A. was supported by the National Science Foundation (NSF 151548) and by the Roy J. Carver Chair in Neuroscience.

CONFLICTS OF INTEREST

The authors declare that there are no competing interests.

ORCID

Anne Günther  <https://orcid.org/0000-0001-8081-9275>

Vincent Luczak  <https://orcid.org/0000-0001-8747-9429>

Ted Abel  <https://orcid.org/0000-0003-2423-4592>

Arnd Baumann  <https://orcid.org/0000-0001-9456-7275>

REFERENCES

- Wahl-Schott C, Biel M. HCN channels: structure, cellular regulation and physiological function. *Cell Mol Life Sci CMLS*. 2009;66:470-494.
- Ludwig A, Zong X, Jeglitsch M, Hofmann F, Biel M. A family of hyperpolarization-activated mammalian cation channels. *Nature*. 1998;393:587-591.
- Santoro B, Grant SG, Bartsch D, Kandel ER. Interactive cloning with the SH3 domain of N-src identifies a new brain specific ion channel protein, with homology to Eag and cyclic nucleotide-gated channels. *Proc Natl Acad Sci U S A*. 1997;94:14815-14820.
- Santoro B, Liu DT, Yao H, et al. Identification of a gene encoding a hyperpolarization-activated pacemaker channel of brain. *Cell*. 1998;93:717-729.
- Biel M, Wahl-Schott C, Michalakis S, Zong X. Hyperpolarization-activated cation channels: from genes to function. *Physiol Rev*. 2009;89:847-885.
- Huang Z, Lujan R, Martinez-Hernandez J, Lewis AS, Chetkovich DM, Shah MM. TRIP8b independent trafficking and plasticity of adult cortical pre-synaptic HCN1 channels. *J Neurosci*. 2012;32:14835-14848.
- Piskorowski R, Santoro B, Siegelbaum SA. TRIP8b splice forms act in concert to regulate the localization and expression of HCN1 channels in CA1 pyramidal neurons. *Neuron*. 2011;70:495-509.
- Santoro B, Piskorowski RA, Pian P, Hu L, Liu H, Siegelbaum SA. TRIP8b splice variants form a family of auxiliary subunits that regulate gating and trafficking of HCN channels in the brain. *Neuron*. 2009;62:802-813.
- Halliwel JV, Adams PR. Voltage-clamp analysis of muscarinic excitation in hippocampal neurons. *Brain Res*. 1982;250:71-92.
- Maccaferri G, Mangoni M, Lazzari A, DiFrancesco D. Properties of the hyperpolarization-activated current in rat hippocampal CA1 pyramidal cells. *J Neurophysiol*. 1993;69:2129-2136.
- He C, Chen F, Li B, Hu Z. Neurophysiology of HCN channels: from cellular functions to multiple regulations. *Prog Neurobiol*. 2014;112:1-23.
- Moosmang S, Biel M, Hofmann F, Ludwig A. Differential distribution of four hyperpolarization-activated cation channels in mouse brain. *Biol Chem*. 1999;380:975-980.
- Notomi T, Shigemoto R. Immunohistochemical localization of Ih channel subunits, HCN1-4, in the rat brain. *J Comp Neurol*. 2004;471:241-276.
- Santoro B, Chen S, Luthi A, et al. Molecular and functional heterogeneity of hyperpolarization-activated pacemaker channels in the mouse CNS. *J Neurosci*. 2000;20:5264-5275.
- Dougherty KA, Nicholson DA, Diaz L, et al. Differential expression of HCN subunits alters voltage-dependent gating of h-channels in CA1 pyramidal neurons from dorsal and ventral hippocampus. *J Neurophysiol*. 2013;109:1940-1953.
- Magee JC. Dendritic hyperpolarization-activated currents modify the integrative properties of hippocampal CA1 pyramidal neurons. *J Neurosci*. 1998;18:7613-7624.
- Magee JC. Dendritic Ih normalizes temporal summation in hippocampal CA1 neurons. *Nat Neurosci*. 1999;2:508-514.
- Vaidya SP, Johnston D. Temporal synchrony and gamma-to-theta power conversion in the dendrites of CA1 pyramidal neurons. *Nat Neurosci*. 2013;16:1812-1820.
- Kim CS, Chang PY, Johnston D. Enhancement of dorsal hippocampal activity by knockdown of HCN1 channels leads to anxiolytic- and antidepressant-like behaviors. *Neuron*. 2012;75:503-516.
- Lewis AS, Vaidya SP, Blaiss CA, et al. Deletion of the HCN channel auxiliary subunit TRIP8b impairs hippocampal Ih localization and function and promotes antidepressant behavior in mice. *J Neurosci*. 2011;31:7424-7440.
- Li S, He Z, Guo L, Huang L, Wang J, He W. Behavioral alterations associated with a down regulation of HCN1 mRNA in hippocampal cornu Ammon 1 region and neocortex after chronic incomplete global cerebral ischemia in rats. *Neuroscience*. 2010;165:654-661.
- Nolan MF, Malleret G, Dudman JT, et al. A behavioral role for dendritic integration: HCN1 channels constrain spatial memory and plasticity at inputs to distal dendrites of CA1 pyramidal neurons. *Cell*. 2004;119:719-732.
- Matt L, Michalakis S, Hofmann F, et al. HCN2 channels in local inhibitory interneurons constrain LTP in the hippocampal direct perforant path. *Cell Mol Life Sci CMLS*. 2011;68:125-137.
- Nolan MF, Dudman JT, Dodson PD, Santoro B. HCN1 channels control resting and active integrative properties of stellate cells from layer II of the entorhinal cortex. *J Neurosci*. 2007;27:12440-12451.
- Herrmann S, Schnorr S, Ludwig A. HCN channels--modulators of cardiac and neuronal excitability. *Int J Mol Sci*. 2015;16:1429-1447.
- Baruscotti M, Bucchi A, Viscomi C, et al. Deep bradycardia and heart block caused by inducible cardiac-specific knockout of the pacemaker channel gene Hcn4. *Proc Natl Acad Sci U S A*. 2011;108:1705-1710.
- Harzheim D, Pfeiffer KH, Fabritz L, et al. Cardiac pacemaker function of HCN4 channels in mice is confined to embryonic development and requires cyclic AMP. *EMBO J*. 2008;27:692-703.
- Herrmann S, Stieber J, Stöckl G, Hofmann F, Ludwig A. HCN4 provides a "depolarization reserve" and is not required for heart rate acceleration in mice. *EMBO J*. 2007;26:4423-4432.
- Stieber J, Herrmann S, Feil S, et al. The hyperpolarization-activated channel HCN4 is required for the generation of pacemaker action potentials in the embryonic heart. *Proc Natl Acad Sci U S A*. 2003;100:15235-15240.
- Hughes DI, Boyle KA, Kinnon CM, et al. HCN4 subunit expression in fast-spiking interneurons of the rat spinal cord and hippocampus. *Neuroscience*. 2013;237:7-18.
- Girod A, Ried M, Wobus C, et al. Genetic capsid modifications allow efficient re-targeting of adeno-associated virus type 2. *Nat Med*. 1999;5(9):1052-1056.
- Xiao X, Li J, Samulski RJ. Production of high-titer recombinant adeno-associated virus vectors in the absence of helper adenovirus. *J Virol*. 1998;72:2224-2232.
- Patel TP, Gullotti DM, Hernandez P, et al. An open-source toolbox for automated phenotyping of mice in behavioral tasks. *Front Behav Neurosci*. 2014;8:349.
- Much B, Wahl-Schott C, Zong X, et al. Role of subunit heteromerization and N-linked glycosylation in the formation of functional hyperpolarization-activated cyclic nucleotide-gated channels. *J Biol Chem*. 2003;278:43781-43786.
- Li C-H, Zhang Q, Teng B, Mustafa SJ, Huang J-Y, Yu H-G. Src Tyrosine kinase alters gating of hyperpolarization-activated HCN4 pacemaker channel through Tyr531. *Am J Physiol*. 2008;294:355-362. <https://doi.org/10.1152/ajpcell.00236.2007>.
- Aponte Y, Lien C-C, Reisinger E, Jonas P. Hyperpolarization-activated cation channels in fast-spiking interneurons of rat hippocampus. *J Physiol*. 2006;574:229-243.
- Hegle AP, Nazzari H, Roth A, Angoli D, Accili EA. Evolutionary emergence of N-glycosylation as a variable promoter of HCN channel surface expression. *Am J Physiol Cell Physiol*. 2010;298:C1066-C1076.
- Zha Q, Brewster AL, Richichi C, Bender RA, Baram TZ. Activity-dependent heteromerization of the hyperpolarization-activated, cyclic-nucleotide gated (HCN) channels: role of N-linked glycosylation. *J Neurochem*. 2008;105:68-77.

39. Zhang Q, Huang A, Lin Y-C, Yu H-G. Associated changes in HCN2 and HCN4 transcripts and if pacemaker current in Myocytes. *Biochim Biophys Acta*. 2009;1788:1138-1147.
40. Günther A, Luczak V, Abel T, Baumann A. Caspase-3 and GFAP as early markers for apoptosis and astrogliosis in shRNA-induced hippocampal cytotoxicity. *J Exp Biol*. 2017;220:1400-1404.
41. Ying S-W, Jia F, Abbas SY, Hofmann F, Ludwig A, Goldstein PA. Dendritic HCN2 channels constrain glutamate-driven excitability in reticular thalamic neurons. *J Neurosci*. 2007;27:8719-8732.
42. Kaupp UB, Seifert R. Molecular diversity of pacemaker ion channels. *Annu Rev Physiol*. 2001;63:235-257.
43. Aschauer DF, Kreuz S, Rumpel S. Analysis of transduction efficiency, tropism and axonal transport of AAV serotypes 1, 2, 5, 6, 8 and 9 in the mouse brain. *PLoS One*. 2013;8:e76310.
44. Shepherd JK, Grewal SS, Fletcher A, Bill DJ, Dourish CT. Behavioural and pharmacological characterisation of the elevated “zero-maze” as an animal model of anxiety. *Psychopharmacology*. 1994;116:56-64.
45. Prut L, Belzung C. The open field as a paradigm to measure the effects of drugs on anxiety-like behaviors: a review. *Eur J Pharmacol*. 2003;463:3-33.
46. Hansen RT, Conti M, Zhang H-T. Mice deficient in phosphodiesterase-4A display anxiogenic-like behavior. *Psychopharmacology*. 2014;231:2941-2954.
47. Zhang H-T, Huang Y, Masood A, et al. Anxiogenic-like behavioral phenotype of mice deficient in phosphodiesterase 4B (PDE4B). *Neuropsychopharmacol Off Publ Am Coll Neuropsychopharmacol*. 2008;33:1611-1623.
48. Shishkina GT, Kalinina TS, Dygalo NN. Attenuation of α 2A-adrenergic receptor expression in neonatal rat brain by RNA interference or antisense oligonucleotide reduced anxiety in adulthood. *Neuroscience*. 2004;129:521-528.
49. Wang M, Ramos BP, Paspalas CD, et al. α 2A-Adrenoceptors strengthen working memory networks by inhibiting cAMP-HCN channel signaling in prefrontal cortex. *Cell*. 2007;129:397-410.
50. Arnsten AFT, Paspalas CD, Gamo NJ, Yang Y, Wang M. Dynamic network connectivity: a new form of neuroplasticity. *Trends Cogn Sci*. 2010;14:365-375.
51. Brager DH, Lewis AS, Chetkovich DM, Johnston D. Short- and long-term plasticity in CA1 neurons from mice lacking h-channel auxiliary subunit TRIP8b. *J Neurophysiol*. 2013;110:2350-2357.
52. Han Y, Heuermann RJ, Lyman KA, Fisher D, Ismail Q-A, Chetkovich DM. HCN channel dendritic targeting requires bipartite interaction with TRIP8b and regulates antidepressant-like behavioral effects. *Mol Psychiatry*. 2017;22:458-465.
53. Heuermann RJ, Jaramillo TC, Ying S-W, et al. Reduction of thalamic and cortical Ih by deletion of TRIP8b produces a mouse model of human absence epilepsy. *Neurobiol Dis*. 2016;85:81-92.
54. Lewis AS, Schwartz E, Chan CS, et al. Alternatively spliced isoforms of TRIP8b differentially control h channel trafficking and function. *J Neurosci*. 2009;29:6250-6265.
55. Zobeiri M, Chaudhary R, Datunashvili M, et al. Modulation of thalamo-cortical oscillations by TRIP8b, an auxiliary subunit for HCN channels. *Brain Struct Funct*. 2018;223:1537-1564.
56. Zolles G, Wenzel D, Bildl W, et al. Association with the auxiliary subunit PEX5R/Trip8b controls responsiveness of HCN channels to cAMP and adrenergic stimulation. *Neuron*. 2009;62:814-825.
57. Kusch J, Thon S, Schulz E, et al. How subunits cooperate in cAMP-induced activation of homotetrameric HCN2 channels. *Nat Chem Biol*. 2012;8:162-169.
58. Han Y, Noam Y, Lewis AS, et al. Trafficking and gating of hyperpolarization-activated cyclic nucleotide-gated channels are regulated by interaction with tetratricopeptide repeat-containing Rab8b-interacting protein (TRIP8b) and cyclic AMP at distinct sites. *J Biol Chem*. 2011;286:20823-20834.
59. Lyman KA, Han Y, Heuermann RJ, et al. Allosteric between two binding sites in the ion channel subunit TRIP8b confers binding specificity to HCN channels. *J Biol Chem*. 2017;292:17718-17730.
60. Wilkars W, Liu Z, Lewis AS, et al. Regulation of axonal HCN1 trafficking in perforant path involves expression of specific TRIP8b isoforms. *PLoS One*. 2012;7:e32181.

SUPPORTING INFORMATION

Additional supporting information may be found online in the Supporting Information section at the end of the article.

How to cite this article: Günther A, Luczak V, Gruteser N, Abel T, Baumann A. HCN4 knockdown in dorsal hippocampus promotes anxiety-like behavior in mice. *Genes, Brain and Behavior*. 2019;18:e12550. <https://doi.org/10.1111/gbb.12550>